Subduction geometry beneath south-central Alaska and its relationship to volcanism

Robert Martin-Short[1], Richard M. Allen[1], Ian D. Bastow[2]

[1]U.C. Berkeley Seismological Laboratory

[2]Department of Earth Science and Engineering, Imperial College London.

Corresponding author: Robert Martin-Short (rmartin-short@berkeley.edu)

Key Points:

- **Dense seismic deployment in Alaska provides most complete images of the subducted Pacific-Yakutat slab to date.**
- **Evidence for subduction beneath the Wrangell Volcanoes in Central Alaska is lacking, implying an alternative source of magmatism there.**
- **Subduction of thickened Yakutat crust causes shallow slab flattening and a dearth of volcanism, but deeper slab geometry is un-altered.**

Abstract

The southern Alaskan margin captures a transition between compression and strike-slip dominated deformation, accretion of the over-thickened Yakutat terrane, termination of Aleutian arc magnetism and the enigmatic Wrangell Volcanic Field. The extent of subduction and mantle structure below this region is uncertain, with important implications for volcanism. We present compressional- and shear-wave mantle velocity models below south-central Alaska that leverage a new seismometer deployment to produce the most complete image of the subducting Pacific-Yakutat plate to date. We image a steeply-dipping slab extending below central Alaska to >400km depth, which abruptly terminates east of ~145ºW. There is no significant slab anomaly beneath the nearby Wrangell volcanoes. A paucity of volcanism is observed above the subducting Yakutat terrane, but the slab structure below 150km depth and Wadati-Benioff zone here are similar to those along the Aleutian-Alaska arc. Features of the mantle wedge or overlying lithosphere are thus responsible for the volcanic gap.

1. Introduction

South-central Alaska, at the northeastern vertex of the Pacific plate, displays a so-called 'corner geometry'. Here, the Pacific plate is bounded to the west by the Queen Charlotte/Fairweather transform system and to the north by the Alaska-Aleutian subduction zone (Figure 1: e.g. Plafker & Berg 1994; Eberhart-Phillips et al., 2006). Subduction began in the Late Cretaceous, with consumption of the Kula plate. This was followed by subduction of the Pacific plate, after its capture of Kula at 40-45 Ma (Madsen et al., 2006). This long history of subduction has resulted in growth of northwestern North America though the accretion of oceanic and island arc terrains to form what is now south-central Alaska (Plafker & Berg 1994).

Today, the strike of the Alaska-Aleutian subduction zone rotates from approximately normal to plate motion in the central Aleutians into an oblique orientation below Alaska, where it appears to terminate (Ratchkovski & Hansen 2002). The situation is further complicated by the presence of the Yakutat terrane, a region of thick (>20km) oceanic crust that lies at the eastern terminus of the subduction zone and is in the process of being accreted to the Alaskan margin (Plafker & Berg 1994). Convergence of the Yakutat terrane is believed to be responsible for many unusual features of the subduction zone beneath south-central Alaska. These include the very shallow Wadati-Benioff Zone (WBZ) out to 600km from the trench, broad intraplate deformation, rapid uplift of the Chugach and Alaska ranges and a paucity in volcanism above the inferred subducted extent of the Yakutat terrane, known as the Denali gap (Wang & Tape 2014, Nye 1999). High resolution imaging of the mantle below the Denali gap and the adjacent volcanogenic arc is required to better understand the differences in slab geometry and extent between them.

Another unusual feature of south-central Alaska is the Wrangell Volcanic Field (WVF), a group of volcanoes that lie close to the eastern edge of the subducting Yakutat terrane (Figure 1). These volcanoes extend ~200km from the Alaska-Yukon border. They exhibit a northwestward progression in activity, commencing ~26Mya and subsiding since ~0.2Mya (Richter et al., 1990; Finzel et al. 2011). Given the scarcity of earthquake activity below 50km depth beneath the WVF, the existence of a subducting slab beneath this area and its relationship to volcanism have become topics of significant debate. The tomographic study of Tian & Zhao (2012) suggests the presence of a deep slab beneath the WVF, implying a connection between magnetism and slab dehydration. In contrast, the geodynamic work of Jadamec & Billen (2012) suggests that WVF volcanism might instead be driven by toroidal flow and mantle upwelling around a more easterly slab-edge. Such a feature would be expected to produce a near-vertical, low velocity anomaly below the WVF, but seismic tomographic images of the region to-date are either of insufficient depth-extent (e.g. Wang & Tape, 2014) or data coverage (e.g. Qi et al. 2007) to illuminate it.

Although the shallow structure below south-central Alaska is relatively well imaged, the geometry of the deep slab (below 100km), its potential relationship to enigmatic volcanism in the WVF and its role in the creation of the Denali gap are poorly known. Here we present teleseismic P- and S-wave models of south-central Alaska, which provide the most complete image of the deep slab structure to date. We ar[illegible]e to confidently image a steeply dipping Pacific-Yakutat slab down to below 400km de[illegible]bserve a sharp termination of the subduction zone and see no evidence for a deep slab beneath the WVF. Despite being hinted at by previous studies, these findings have only been made possible by the recent deployment of Transportable Array (TA) seismometers in Alaska, which has significantly expanded network coverage and hence increased the size of the region that we can confidently image with tomographic techniques (Figure S1). Thus, our study represents some of the first scientific findings in this major community effort to understand the seismotectonics of Alaska.

2. Background and previous studies

Initial studies of the crustal and mantle structure in Alaska made use of the region's abundant seismicity to investigate the geometry of the subducting plate (e.g. Page et al., 1989; Ratchkovski & Hansen 2002). Local seismicity has also been used in body wave tomography studies, which have focused mainly on the shallow structure of the slab, mantle wedge and continental crust (e.g. Zhao et al., 1995, Tian & Zhao 2012). The subducting Pacific-Yakutat slab is consistently imaged as a dipping, high velocity structure, whose upper surface is delineated by intense seismic activity to ~150km depth (Eberhart-Phillips et al., 2006). The dip of the down-going slab shallows beneath the Denali gap (Figure 2: e.g., Hayes et al., 2012). Furthermore, a distinct, thin (<20km), low velocity layer is imaged directly above the high velocity slab in this region, with seismicity occurring solely within this feature (Ferris et al., 2003; Eberhart-Phillips et al., 2006). Rondenay et al. (2008) report that the low velocity layer appears to become thinner with depth, and disappears below 150km. It is interpreted to be the thick, hydrated, Yakutat crust, which undergoes dehydration and phase transformation to eclogite at depth (Hacker et al., 2003). The 15-20km thickness of this layer, as inferred from the images of Rondenay et al. (2008), is in excellent agreement with Yakutat crustal thickness estimates from offshore reflection studies (Christeson et al., 2010; Worthington et al., 2012).

The Yakutat terrane likely formed as an oceanic plateau offshore of the American Pacific Northwest, and has since been rafted into its present location by motion of the Queen-Charlotte/Fairweather fault system (Worthington et al., 2012). Convergence of this thick oceanic crust has been ongoing for at least 23 Ma (Finzel et al., 2011), during which time it has penetrated over 600km inland of the trench (Eberhart-Phillips et al., 2006). Figure 1 shows the striking correlation between the subducted Yakutat region and the 400km long 'gap' in volcanism from Hayes Volcano to Buzzard Creek Maars, known as the Denali volcanic gap

(Nye, 1999). It is likely that shallow subduction of thick, buoyant, Yakutat crust is responsible for this phenomenon. However, the exact causes of the Denali gap are not well understood, in part because the slab here does not lie flat against the continental lithosphere and the mantle wedge below the volcanic gap appears suitable for melt production (Rondenay et al., 2010).

Magmatism at the WVF has been the subject of multiple petrological and tectonic studies. Lavas sampled from this region feature alkaline, transitional and calc-alkaline affinities, suggesting a range of contributing sources (Skulski et al., 1991). The oldest eruptive centers, which lie in the southeast, feature mainly alkaline and transitional lavas. Those in the northwest feature lavas with a transitional and calc-alkaline affinity, from which various studies have inferred the presence of a subducting slab at depth beneath the region (e.g. Page et al., 1989, Skulski et al., 1991). However, the presence of adakite lavas at Mounts Drum and Churchill has also been used to argue for flat subduction and slab melting beneath the WVF (Preece & Hart 2004).

Tomographic imaging studies of the type previously used to image the aforementioned regions generally make use of local events, thus constraining only relatively shallow (<100km) velocity structure; there have been relatively few teleseismic studies. Using surface-wave tomography, Wang & Tape (2014) imaged the slab as an elongate, high velocity anomaly with abrupt termination at ~64°N, 146°W. However, their technique only provides good resolution above 200km depth. Qi et al. (2007) produced a teleseismic P-wave mantle velocity model for the region that reveals structure to 700km depth, but used a much sparser seismic network than is available today.

3. Methodology

The models presented here are produced using the method of finite frequency, travel-time tomography, featuring the joint inversion of two frequency bands for P-waves and one for S-waves. The workflow is similar to that employed for the 'Dynamic North America' (DNA) models (Obrebski et al., 2010; Obrebski et al., 2011; Porritt et al., 2014). The waveforms of earthquakes with Mw > 6.0 and epicentral distances of 30-120º from the center of the array were obtained for the period January 2014 to June 2016. This yielded 288 earthquakes recorded at up to 158 stations (Figure 1). The data were instrument-corrected and rotated into the tangential-radial-vertical coordinate frame: P-wave arrival times were picked on the vertical component and S-waves on the tangential. Travel time residuals were calculated with reference to the IASP91 travel-time tables (Kennett & Engdahl 1991) and refined using the multichannel cross correlation method of (VanDecar & Crosson 1990). Refined delay times were determined for frequency bands of 0.02-0.1Hz and 0.9-1.2Hz for the P waves, and 0.02-0.1Hz for the S waves. These filter bands produce the highest signal to noise ratio, based on visual inspection of the waveforms. In our tomography workflow, the travel time sensitivity of the wavefield for each event is approximated using finite frequency kernels calculated using the paraxial method of Hung et al. (2000), which provide a better representation of the three-dimensional (3D) wavefield than infinite-frequency rays (Hung et al., 2001; Maceira et al., 2015). The kernels and delay times are then assembled into a linear system, which is solved using the method of damped least squares. A model of velocity perturbations is then recovered. Our method simultaneously inverts for a vector of slowness perturbations at each of the grid cells, plus station and event static corrections to account for unresolvable near-surface structure and event-specific biases in the delay times, respectively (Text S1).

The model grid is defined over a spherical cap spanning 166.3ºW/53.0ºN to 115.7ºW/71.0ºN, with a latitudinal node spacing of 0.28º, a longitudinal spacing of 0.8º and a vertical spacing of 15km. The grid extends from the surface to 1000km depth. The volume encompassed by our grid is much larger than the region where we expect to have good resolution: This corresponds to the region covered by the main cluster of stations, to ~500km depth. The number of crossing raypaths is limited at greater depths.

4. Resolution tests

We test the resolving power of our dataset in two ways: firstly, a standard checkerboard test employed with progressively smaller checkers to determine the characteristic length scale of the smallest recoverable anomalies (Figure S2), and a 'synthetic slab' test (Figure S3). Normally-distributed errors with standard deviation 0.1s are added to the synthetic travel-time data, which are then inverted using the same regularization scheme as for the observed data.

The checkerboard tests indicate that our P- and S-wave models have good resolution of features on the scale of the subducting slab to ~400km depth. Resolution is best beneath south-central Alaska and quickly depreciates towards the edges of the seismometer array. Good recovery of features with lateral scales of 100km is seen in the models at 100km depth, and this transitions to a recovery of features with lateral scales of ~300km at 400km depth, as indicated by Supporting information S3.

The synthetic slab tests are created using three, 100km thick artificial anomalies of +4%, which dip at 50º, terminate at 250km depth and strike in the approximate orientation expected for the Pacific-Yakutat-Wrangell slab (e.g. Jadamec & Billen 2012). The pattern of anomalies east of Cook Inlet is successfully recovered, implying that our dataset is able to image slab-like features in the region of greatest tectonic interest: That is, the transition between the Aleutian Island arc into the Denali gap, the Yakutat subduction region and the mantle beneath the WVF. Importantly, these synthetic tests suggest that if a deep slab were present beneath the WVF, we would resolve it.

5. Results

We present our P and S-wave velocity perturbation models in a series of depth slices (Figure 2), cross sections (Figure 3) and 3D renderings (Figure S5, Movie S1). The most striking aspect of our models is the presence of an elongate, dipping, high velocity feature that extends northeastwards from Cook Inlet into central Alaska, where it terminates abruptly. This is interpreted to be the subducting Pacific-Yakutat slab. The slab is known to continue further west below the Aleutian Island arc but is not seen in our model because of the lack of resolution in that region, as indicated by the synthetic tests.

The strike of the slab-related anomaly is only subparallel to that of the trench, meaning that it advances inland of the trench from west to east. The strike of this feature exhibits excellent alignment with the northwestern edge of the of subducted Yakutat crust, and it terminates just to the northeast of the northernmost extent of Yakutat subduction (Figure 2). Furthermore, the slab anomaly is well aligned with the WBZ, which provides strong support for our interpretation of it as subducting lithosphere (Figure 2).

Along the northernmost section of the slab, beneath the Denali gap, seismicity extends to a maximum depth of approximately 150km. However, our models indicate that the slab continues to a much greater depth, likely below 400km (Figure 2). This is consistent with the region's long history of subduction, and with the earlier tomography study of Qi et al. (2007). West of the Denali gap the WBZ extends slightly deeper, and the slab is also seen to depths of ≥400km.

At its northeastern-most corner, the high velocity anomaly associated with the slab extends to about 150km beyond the furthest extent of the seismicity (Figure 2a). This is a surprising finding given the apparent strong connection between seismic activity and slab presence elsewhere in the region. The feature was also highlighted by Wang & Tape (2014), and its presense in our body wave tomography supports their assertion that the Pacific-Yakutat slab extends further northeast than would be predicted based on the WBZ alone.

The profile of the slab changes along strike (Figure 3). Below the Denali gap, it is shallow for approximately 500km between the trench and the northwestern edge of the subducted Yakutat terrane, where it lies at a depth of about 150km (Figure 3b). Beyond this, the deep slab exhibits a much steeper dip. Furthermore it becomes increasingly steep towards the northeastern-most edge, where it is almost vertical (Figure 2; Figure S5). Below the volcanic region, the slab exhibits a similar profile in both P- and S- wave profiles, but with a shorter zone of shallow subduction and a more gradual transition into a steep subduction at depth (Figures 2 and 3)

Figure 3a demonstrates that the Wrangell volcanoes are not underlain by a deep, high velocity structure. Our resolution tests (Figures S2-S4) suggest that if such a feature were present, it would be clearly imaged. Thus, we can confidently state that there is an abrupt and significant change in upper mantle velocity structure between the Denali gap and the WVF.

6. Discussion

Our models provide new constraints on the geometry of the deep slab beneath Alaska, its relationship with the Denali volcanic gap and its proximity to the WVF. In the following section, we examine each of these regions in turn and make new tectonic interpretations based on the tomographic images.

6.1 Denali Gap and the Yakutat terrane

Our models provide insight into the similarities and differences between the geometry of subduction within and outside of the Denali volcanic gap: the slab extends to >400km depth beneath both regions (Figures 2 and 3). However, vertical smearing revealed by our resolution tests prevents an accurate determination of the maximum slab depth in these models (Figures S3, S4). Nevertheless, given that subduction has been continuous in this region for >100 My, several thousand kilometers of lithosphere must have descended here and thus a deep slab is to be expected (Plafker & Berg 1994).

The shallow portion of the slab within the Denali gap, which bears the over-thickened Yakutat crust, dips at a shallow angle of ~30º to ~100km depth, where it steepens to ~60º (Figure 3b). This behavior is indicated by the WBZ (Ratchkovski & Hansen, 2002). Beyond the northwestern edge of the subducted Yakutat region the slab dips steeply into the mantle all the way along the Denali gap. The dip increases towards the northeastern corner, where the slab is almost vertical. This is consistent with the observations of Lallemend et al. (2005), who note an increase in slab dip with edge proximity at many subduction zones. This phenomenon could be attributed to localized heating of the lithosphere near the slab edge, which facilitates bending and steepening when the slab is continuous to great depths.

If we accept that the region identified by Eberhart-Phillips et al. (2006) represents the true extent of the subducted Yakutat crust, then it follows that much of the slab material seen in our models beneath the Denali gap was subducted prior to Yakutat collision. Hence, it is Pacific lithosphere that once existed between the incoming Yakutat block and the Alaskan margin. Evidently, the Yakutat collision initiated a northwestward propagating zone of flat-slab subduction beneath the Denali gap but the flattened Yakutat portion remained connected to the older, steeper, Pacific portion. The effects of the Yakutat subduction at shallow depth may also have encouraged steepening of the deeper part of the slab. Time-dependent, three-dimensional modeling of the situation would be required to test this hypothesis.

Seismic imaging studies of the Yakutat terrane suggest that it subducts to ~150km depth beneath the Denali gap (e.g. Ferris et al, 2003; Rondenay et al., 2008). These studies also reveal that seismic activity is concentrated within the descending Yakutat crust. Our images suggest that the WBZ lies close to the uppermost surface of the subducting slab below the Denali gap and terminates at ~150km. Accordingly, seismic activity is particularly intense in the 100-150km-depth range (Figure 3b). These observations support the suggestion that these intermediate depth earthquakes are generated by dehydration reactions in the basaltic Yakutat crust, which transforms to eclogite within this depth range (Hacker, et al., 2003). The presence of dehydration-related seismic activity here has important implications for the possible causes of the Denali volcanic gap: it implies that the mantle wedge is hydrated. Thermal modeling studies predict that mantle wedge temperatures here should exceed the wet-solidus of peridotite, allowing melt generation (Rondenay et al., 2008). Thus implies that there must be some feature of the Denali gap region that prevents mantle wedge melt from reaching the surface and erupting as volcanoes as it does along the Aleutian Island arc.

Rondenay et al (2010) propose a model to explain the paucity of volcanism in the Denali Gap, whereby the advancing shallow subduction of the Yakutat terrane cools the mantle wedge system and prevents melt from accumulating in a ‘pinch zone’ where it can feed volcanism. Instead, the melt is proposed to accumulate in a more diffuse region at the top of the mantle wedge, simultaneously explaining a low velocity anomaly imaged there (Rondenay et al., 2008). An alternative hypothesis suggests that melt is present in the mantle wedge, but is unable to migrate to the surface due to the compressional regime that exists within the crust between the megathrust and the Denali fault system (McNamara & Pasyanos., 2002). The resolution of our tomography models is insufficient to discern features of the continental crust or shallow mantle wedge, although it is intriguing that high velocity anomalies and more abundant seismic activity are observed in the mantle wedge below the Denali gap (Figure 3b) whereas this is not the case beneath the volcanic region (Figure 3c). This could hint at a cooler mantle wedge beneath the Denali gap, but additional imaging constraints from surface waves or local seismicity would be required to substantiate this.

6.2 Volcanic arc

Figure 3c shows a cross section through the eastern end of the Aleutian-Alaskan arc, near Mt Spurr, a stratovolcano typical of this chain. Here, the WBZ lies along the uppermost surface of the descending slab, before terminating at ~ 200km depth. This suggests that seismic activity here is mainly due to dehydration of the subducted oceanic crust (Hacker et al. 2003). The slab profile is very similar to that for the Denali Gap region (Figure 3b), although the length of shallow, low-angle subduction is smaller (<200km), near-surface earthquake activity is less abundant and there are no high velocity anomalies in the mantle wedge. Volcanic activity is generally located above the 100km slab depth contour, implying the existence of a hydrated mantle wedge and migration pathways for melt to reach the surface.

6.3 Wrangell slab

We observe a continuous curtain of subducted material from the Aleutian Island arc into central Alaska, but one that terminates at ~145°W instead of continuing below the Wrangell volcanoes (Figure 2). This geometry is similar to that predicted by Jadamec & Billen (2010) based on numerical modeling of the mantle flow field around the slab edge and comparison with observations of seismic anisotropy (e.g. Christensen & Abers, 2010). The preferred model of Jadamec & Billen (2010) features a 325km deep Pacific-Yakutat slab that terminates at 148°W but is connected to a much shorter Wrangell slab that extends down to 125km. The presence of this sharp slab edge is predicted to generate a toroidal flow pattern and mantle upwelling beneath the WVF, which led Jadamec & Billen (2010, 2012) to suggest that volcanism here could be driven by this upwelling. Our models support this interpretation to the extent that we see no evidence for a slab beneath the Wrangell volcanoes, implying that activity there must have some other source (Figure 3a). We also see several vertically-continuous low velocity anomalies within close proximity to the WVF, which may tentatively be linked to mantle upwelling.

Finzel et al. (2011) propose a further explanation for Wrangell volcanism, which may also be consistent with our images. The northwestward younging of Wrangell volcanic belt strata and its close proximity to the eastern edge of the subducted Yakutat terrane implies some connection to the low-angle insertion of the Yakutat crust beneath North America. A combination of magmatism along extensional strike-slip faults and partial melting of the Yakutat slab edge could be invoked to explain the spatial variation in the geochemical characteristics of the Wrangells, and imply that a deep slab is not necessary to explain them (Skulski et al. 1991; Finzel et al., 2011).

7. Conclusion

We have presented P- and S-wave finite frequency tomographic models of the mantle beneath South-Central Alaska using data from new seismometer networks. Our models demonstrate for the first time the presence of a deep, continuous slab that extends from Cook Inlet into central Alaska, where it terminates abruptly. Slab dip is shallow where thick Yakutat crust is subducting, but steepens dramatically beyond its northwest boundary. Slab geometry cannot explain the Denali volcanic gap, which thus more likely owes its existence to variations in either mantle wedge characteristics, or the overriding plate (e.g., McNamara & Pasyanos 2002; Rondenay et al. 2010). Evidence for a deep slab beneath the Wrangell volcanoes is lacking, in line with the geodynamic modelling predictions of Jadamec & Billen (2010). An alternative magma source for Wrangell volcanism, such the Yakutat-edge-melting model of Finzel et al. (2011), or the slab-edge upwelling suggestion of Jadamec & Billen (2012) is thus required.

Acknowledgements

This paper benefitted from useful discussions with R. Porritt. Data were sourced from the IRIS Data Management Center, which is funded through the Seismological Facilities for the Advancement of Geoscience and EarthScope (SAGE) Proposal of the National Science Foundation under Cooperative Agreement EAR-1261681. The program obpyDMT (Hosseini, 2015) was used to download the seismic waveforms. Figures were produced using the Generic Mapping Tools (GMT) software (Wessel & Smith, 1998). We intend to upload the tomography model data to an appropriate repository. The authors declare no conflicts of interest.

References

Bird, P., 2003. An updated digital model of plate boundaries.*Geochem Geophys*., 4(3). doi/10.1029/2001GC000252.

Christensen, D.H. & Abers, G. a., 2010. Seismic anisotropy under central Alaska from SKS splitting observations. *J. Geophys. Res.*, 115(B4), 1–12.

Christeson, G.L. et al., 2010. The Yakutat terrane: Dramatic change in crustal thickness across the transition fault, Alaska. *Geology*, 38(10), 895–898.

Ferris, A. et al., 2003. High resolution image of the subducted Pacific (?) plate beneath central Alaska, 50-150 km depth. *Earth Planet. Sci. Lett.*, 214(3-4), 575–588.

Finzel, E.S. et al., 2011. Upper plate proxies for flat-slab subduction processes in southern Alaska. *Earth Planet. Sci. Lett.*, 303(3-4), 348–360.

Gripp, A.E. & Gordon, R.G., 2002. Young tracks of hotspots and current plate velocities. *Geophys. J. Int.*, 150(2), 321–361.

Hacker, B.R. et al., 2003. Subduction factory 2. Are intermediate-depth earthquakes in subducting slabs linked to metamorphic dehydration reactions? *J. Geophys. Res.*, 108, p.2030.

Hayes, G.P., Wald, D.J. & Johnson, R.L., 2012. Slab1.0: A three-dimensional model of global subduction zone geometries. *J. Geophys. Res: Solid Earth*, 117(1), 1–15.

Hosseini, K. (2015), obspyDMT (Version 1.0.0) [software] [https://github.com/kasra-hosseini/obspyDMT]

Jadamec, M. a. & Billen, M.I., 2012. The role of rheology and slab shape on rapid mantle flow: Three-dimensional numerical models of the Alaska slab edge. *J. Geophys. Res: Solid Earth*, 117(2), 1–20.

Kennett, B.L.N. & Engdahl, E.R., 1991. Traveltimes for global earthquake location and phase identification. *Geophys. J. Int.*, 105(2), 429–465.

Madsen, J.K. et al., 2006. Cenozoic to recent plate configurations in the Pacific Basin: Ridge subduction and slab window magmatism in Western North America. *Geosphere*, 2(1), 11–34.

McNamara, D.E., 2002. Seismological evidence for a sub-volcanic arc mantle wedge beneath the Denali volcanic gap, Alaska. *Geophys. Res. Lett.*, 29(16), 2–5.

Obrebski, M. et al., 2011. Lithosphere-asthenosphere interaction beneath the western United States from the joint inversion of body-wave traveltimes and surface-wave phase velocities. *Geophys. J. Int.*, 185(2), 1003–1021.

Obrebski, M. et al., 2010. Slab-plume interaction beneath the Pacific Northwest. *Geophys. Res. Lett.*, 37(14), 1–6.

Page, R. a., Stephens, C.D. & Lahr, J.C., 1989. Seismicity of the Wrangell and Aleutian Wadati-Benioff Zones and the North American Plate along the Trans-Alaska Crustal Transect, Chugach Mountains and Copper River Basin, southern Alaska. *J. Geophys. Res.*, 94(B11), p.16059.

Plafker, G. & Berg, H., 1994. Overview of the geology and tectonic evolution of Alaska. *The Geology of North America*, G-1, The Geology of Alaska, 989–1021.

Porritt, R.W., Allen, R.M. & Pollitz, F.F., 2014. Seismic imaging east of the Rocky Mountains with USArray. *Earth Planet. Sci. Lett.*, 402(C), 16–25.

Preece, S.J. & Hart, W.K., 2004. Geochemical variations in the. *Tectonophysics*, 392(1), pp.165–191.

Qi, C., Zhao, D. & Chen, Y., 2007. Search for deep slab segments under Alaska. *Phys. Earth Planet. Inter.*, 165(1-2), 68–82.

Ratchkovski, N. a. & Hansen, R. a., 2002. New evidence for segmentation of the Alaska subduction zone. *Bull. Seismol. Soc. Am.*, 92(5), 1754–1765.

Richter, DH; Smith, JG; Lanphere, MA; Dalrymple, GB; Reed, BL; Shew, N., 1990. Age progression of volcanism, Wrangell volcnaic field, Alaska. *Bull. Volc.*, 53, 29–44.

Rondenay, S., Montési, L.G.J. & Abers, G. a., 2010. New geophysical insight into the origin of the Denali volcanic gap. *Geophys. J. Int.*, 182(2), pp.613–630.

Skulski, T., Francis, D. & Ludden, J., 1991. Arc-transform magmatism in the Wrangell volcanic belt. *Geology*, 19(1), pp.11–14.

Tian, Y. & Zhao, D., 2012. Seismic anisotropy and heterogeneity in the Alaska subduction zone. *Geophys. J. Int.*, 190(1), pp.629–649.

Vandecar, B.Y.J.C. & Crosson, R.S., 1990. Determination of teleseismic relative phase arrival times using multichannel cross-correlation and least squares. *Bull. Seismol. Soc. Am.*, 80(1), pp.150–169.

Wang, Y. & Tape, C., 2014. Seismic velocity structure and anisotropy of the Alaska subduction zone based on surface wave tomography. *J. Geophys. Res.*, 119(February), pp.1–21.

Wessel, P. & Smith, W.H.F., 1998. New, improved version of generic mapping tools released. *Trans., Am. Geophys. Union*, 79(47), pp.579–579.

Worthington, L.L. et al., 2012. Crustal structure of the Yakutat terrane and the evolution of subduction and collision in southern Alaska *J. Geophys. Res: Solid Earth*, 117(1), pp.1–20.

Zhao, D., Christesen, D. & Pulpan, H., 1995. Tomographic imaging in the Alaska subduction zone. *J. Geophys. Res.*, 100(B4), pp.6487–6504.

Figures

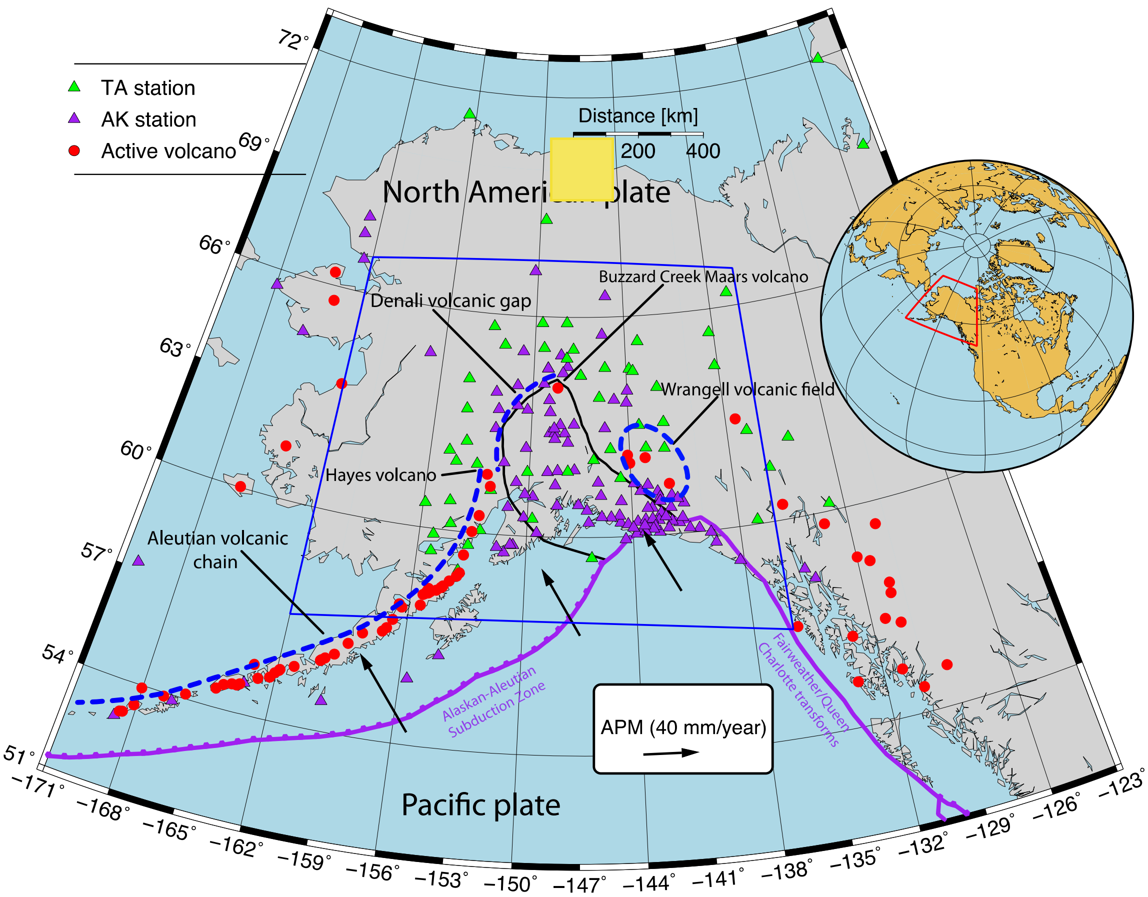

Figure 1. Map showing the distribution of broadband seismometers used in this study (triangles). A total of 158 stations were used in this study. The black line indicates the extent of the subducted Yakutat crust as inferred by Eberhart-Phillips et al (2006). Red dots indicate sites of Holocene volcanic activity, while purple lines indicate plate boundaries (Bird 2003). Black arrows indicate the direction and magnitude of absolute plate motion (APM) from Gripp & Gordon (2002). The blue box outlines the extent of the maps shown in Figure 2.

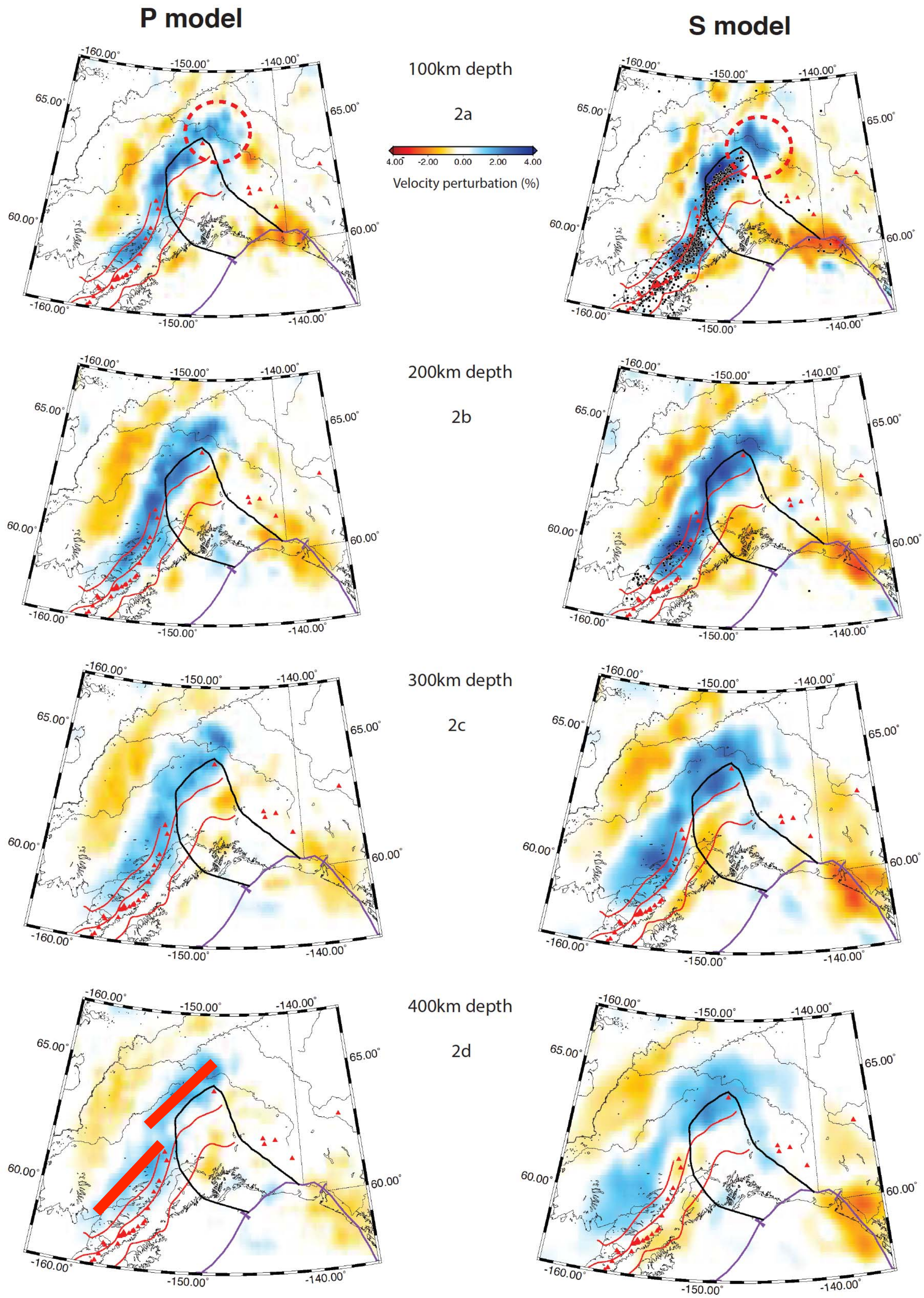
P model
S model
100km depth
2a
200km depth
2b
300km depth
2c
400km depth
2d
Velocity perturbation (%)
4.00
-2.00
0.00
2.00
4.00
-160.00°
-150.00°
-140.00°
65.00°
60.00°

Figure 2: Depth slices though P and S wave tomographic models within the blue box in figure 1. Blue regions indicate high velocity anomalies, which are commonly interpreted to be relatively cold, dense regions of the mantle. These images clearly show the presence of an elongate, high velocity anomaly that dips towards the northwest. This is interpreted to be the subducting Pacific-Yakutat slab. The black line indicates the subducted extent of the Yakutat Terrane from Eberhart-Phillips et al. (2006). Red lines are 50km slab-depth contours from the slab 1.0 model (Hayes et al. 2012). Red triangles are Holocene volcanoes. The red circle in 2a indicates a well-resolved high velocity anomaly that extends significantly to the northeast of the seismicity. Earthquake hypocenters from the Alaska Earthquake Information Center (AEIC) catalog of M>5.0 and within 20km the depth slice are plotted on the S model.

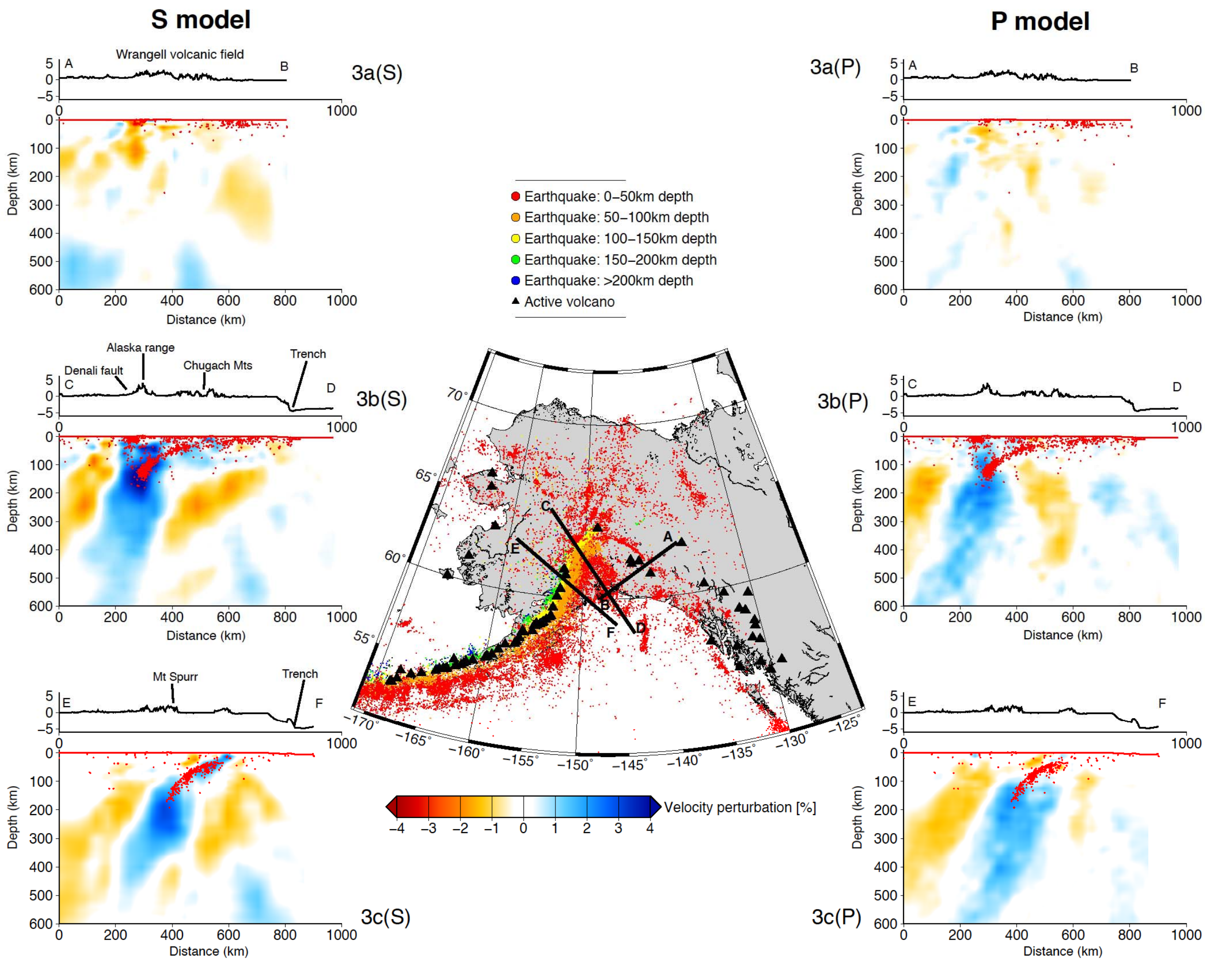

Figure 3: Cross-sections though the tomographic models and topographic relief in three regions of interest: A-B (3a), Wrangell volcanic belt; C-D (3b), Denali volcanic gap; E-F (3c), Volcanogenic region. The hypocenters of earthquakes with M>3.0 with 25km of the sections lines are shown on the cross sections. The locations of all M>3.0 seismicity in Alaska are also shown on the inset map. This earthquake information was obtained from the AEIC catalog.